DEUTSCHES ELEKTRONEN-SYNCHROTRON DESY

DESY SR-82-19
October 1982

PHOTOCONDUCTIVITY AND THE EVOLUTION OF ENERGY BANDS IN FLUID XENON

by

R. Reininger, U. Asaf and I.T. Steinberger

Racah Institute of Physics, The Hebrew University, Jerusalem

V. Saile

HASYLAB, Deutsches Elektronen-Synchrotron DESY, Hamburg

P. Laporte

Equipe de Spectroscopie, C.N.R.S., Saint Etienne

NOTKESTRASSE 85 · 2 HAMBURG 52

To be sure that your preprints are promptly included in the
HIGH ENERGY PHYSICS INDEX ,
send them to the following address (if possible by air mail) :

DESY
Bibliothek
Notkestrasse 85
2 Hamburg 52
Germany

DESY SR-82-19
October 1982

PHOTOCONDUCTIVITY AND THE EVOLUTION OF ENERGY BANDS IN FLUID XENON

R. Reininger, U. Asaf and I.T. Steinberger
Racah Institute of Physics, The Hebrew University, Jerusalem, Israel
and
V. Saile, HASYLAB, Deutsches Elektronen Synchrotron (DESY), 2000 Hamburg 52, Federal Republic of Germany
and
P. Laporte, Equipe de Spectrocopie, C.N.R.S. (LA 171), 158 bis Cours Fauriel, 42023 Saint Etienne, Cedex, France

Abstract

Photoconductivity excitation spectra for densities above 10^{21} atoms/cm^3 up to the triple point exhibit a threshold that moves to lower photon energies with increasing density. Its value extrapolated to zero density is 11.10 eV, i.e. the difference between the energy minimum of the Xe_2^+ molecular ion and the ground state energy of the xenon atom. The hole polarization energy P^+ was evaluated using the Born charging energy for the same density range. These results along with the previously determined values of the electron affinity V_o yielded a full representation of the energy band edges for the whole density range. A multiple-scattering theory of the mobility by Basak and Cohen is used for discussing the results. It is inferred that there is a continous transition from "solid-like" conduction in a conduction band to "gas-like" conduction governed by scattering on distinct atoms. This transition takes place at densities below 10^{21} atoms/cm^3. The relationship between these results and those on the evolution of excitons is also discussed in detail.

to be published in Phys. Rev. B

I. Introduction

In a recent publication[1] we described results on photoresponse in xenon at densities below $\sim 10^{21}$ atoms/cm^3. In this density range the photoelectric current is predominantly due to photoionization even for photon energies less than the ionization energy of the xenon atom (12.12 eV). The photoionization takes place in two steps: upon absorption of a photon the xenon excimer Xe_2^* is formed, followed by spontaneous ionization of the excimer. This involves the formation of the xenon molecular ion Xe_2^+ and a free electron. This essentially atomic process, modified by molecular interactions, is characterized by an excitation spectrum rich in features especially at the lowest densities. The process is possible only above the photon energy threshold of 11.10 eV that is given by the energy differences of the ground state of the molecular ion and the ground state of the free atom. In contrast, the present study deals with higher densities where the photoelectric current is due to photoconductance, its excitation spectrum is almost featureless and may extend to photon energies considerably less than 11.10 eV, depending on the density.

The main facts associating the photoelectric current for number densities $\rho_N > 10^{21}$ atoms/cm^3 with photoconduction are as follows:

a. A photoresponse threshold E_{pc} is observed in liquid xenon at the triple point very near to the photoconductivity threshold of the solid. Its position is consistent with predictions on the change of the band gap based upon the density change at the phase transition[2].

b. The electron mobility[3] μ of liquid xenon near the triple point is very

high, namely 2200 cm^2/volt sec. Its value is about the half of that in solid xenon; this is understood on the basis of the density and compressiblity change at the phase transition[3].

c. Reflection bands due to excitons appear both in solid and liquid xenon[4]. Band gaps calculated from Wannier exciton series are in close agreement with those determined from the photoconductivity threshold.

These facts imply that near the triple point the photoresponse has to be, indeed, attributed to photoconduction proper. For lower densities (down to about 10^{21} atoms/cm^3) the dominance of photoconduction can be surmised from the continuous variation of the mobility[5] and of the energy V_o of the quasi-free electron[6]. Clear evidence that this is, indeed, the case will be presented in this paper.

The exciton bands in fluid xenon were studied for a wide range of densities[7,8]. They were found to be entities different from atomic lines broadened and shifted by molecular interactions, with each exciton band appearing only above its own charcteristic density. Since excitons are closely related to the electron band structure, the above facts raise the question whether there exists a definite density threshold for conduction in a solid-like energy band as well. We note in this context that the zero-field electron mobility μ_o in fluid xenon has a rather deep minimum[5] at a density of about 3×10^{21} atoms/cm^3. This might be interpreted on the basis of the above considerations by regarding the mobility minimum as the threshold for conduction in a solid-like conduction band.

Recent systematic photoinjection studies in fluid xenon[6], krypton[6] and argon[9] gave direct evidence on the energy V_o of a conduction band electron

(in other words, the electron affinity) as a function of density. The results showed that the value of V_o changes continuously and gradually from densities of that of a dilute gas to that of a triple-point liquid, with a minimum in between. Moreover, preliminary results[10] on the density-dependence of the photoconductivity band gap E_{pc}, referring to photon energies below 10.2 eV and densities above 4×10^{21} atoms/cm^3 indicated that E_{pc} varies linearly with density within this range. These facts seem to contradict those quoted above concerning the excitons. The study of photoconductivity excitation spectra in a broad range of densities was undertaken in order to learn whether there is, at any density, a clear threshold for the appearance of a solid-like conduction band or else such conduction develops continuously from conduction in the gas phase. In fact, the experimental results indicated that the development is, indeed, continuous.

The paper also correlates data on the mobility and on the evolution of excitonic bands with the results on E_{pc}. Finally, the energies of the bottom of the conduction band V_o, the top of the valence band V_o-E_{pc}, the hole polarization P^+ and $V_o-E_{pc}+P^+$ are presented as a function of the density, for the first time for any non-metal.

2. Results

The photoconductivity excitation spectra were obtained using monochromated synchrotron radiation from the DORIS storage ring at DESY. The experimental arrangement has been described before [1,10,11] except for the details of the sample cell: it is presented in Fig. 1. The cell was constructed of stainless steel with a copper gasket. The LiF window was glued to one half of a Conflat seal by means of a low-vapour-pressure epoxy resin. For application at low temperatures, a further ring, made of duraluminium, served as substrate for the window, being glued on one side to the Conflat seal and to the window on the other. This ring is not shown in the figure. The inner side of the window accommodated two intertwined gold electrodes prepared by sputtering. Adjacent prongs of the electrodes were spaced at 0.36 mm from each other. High voltage ultra-high vacuum feedthroughs with an interior stainless steel stalk, spring and polished pinhead ensured electrical contact to the gold electrodes.

In the overlapping density range and spectral region these spectra are in full accord with those obtained earlier employing as light source the continuum of a Tanaka lamp filled with krypton or argon. Reflection spectra of the MgF_2-fluid xenon interface were taken near normal incidence using conventional sources, by methods described earlier [4,12].

Figure 2 represents the photocurrent at a fixed voltage as a function of the photon energy for a set of densities. The currents were normalized at each wavelength to the number of photons incident on the xenon gas or fluid per unit time; this number was established by recording the transmission of the LiF window at various temperatures as well as the output

flux of the HONORMI monochromator.

The main feature common to all densities is the onset of photocurrent at a certain photon energy threshold and its persistence at all higher photon energies. The threshold shifts continuously to higher photon energy with decreasing density and simultaneously the initial slope becomes smaller [10]. Crossing the critical isotherm (between graphs c and d) has no effect. At the lowest density presented (curve f) the current level rises considerably again at about 11.0 eV: the broad band seen there (and, less clearly, on curve e as well) is caused by the atomic-molecular photoionization effects discussed previously [1]. At the higher densities (curves a - d) the band is submerged in the higher and broader photoconductivity excitation spectra.

The apparent structure around 8.8 eV is not fully reproducible. At or near this photon energy there is no structure in the reflection spectrum at any density (see Fig. 3), the sample is almost totally transparent and therefore the peak may be associated with photoemission from the rear part of the cell or with impurity photoionization or photoconduction in the sample. In this context we mention that the appearance of the 8.8 eV peak was dependent on the particular epoxy resin used, but this did not influence any one of the other features. In any case there is no doubt that this peak is not intrinsic to the properties of fluid xenon and therefore it will not be discussed further.

More details of the photocurrent excitation spectra can be understood if

these spectra are compared with the corresponding reflectivity spectra. Fig. 3 shows the results of such a comparison for an intermediate density (6.2×10^{21} atoms/cm^3)*. The reflection spectrum exhibits the n = 1 ($\Gamma\ (\frac{3}{2})$) and n' = 1 ($\Gamma\ (\frac{1}{2})$) excitonic peaks at 8.4 and 9.45 eV respectively. The small peak at 10.16 eV can be attributed to transition to the 5d $(\frac{5}{2})^o_3$ level, forbidden in the dilute gas. The peak at 10.32 eV is a band that has developed from the two neighbouring 5d $(\frac{3}{2})^o_1$ and 7s $(\frac{3}{2})^o_1$ states. The reflectivity graph does not extend beyond 10.8 eV, since the measurements were primarily designed to study the evolution of the three lowest energy exciton bands and therefore a MgF_2 front window was employed. The n = 2 ($\Gamma\ (\frac{3}{2})$) Wannier exciton around 9.0 eV is not observed in this graph since this exciton appears[8] only for densities more than 10.8×10^{21} atoms/cm^3. Turning now to the corresponding photocurrent excitation spectrum it should be noted that the reflectivity maximum at 10.32 eV is associated with a decrease in the photocurrent. This feature can be attributed to competition for the incident photons between the band-to-band transitions causing photoconductivity and the discrete transition at 10.32 eV. While for the interband transitions the electrons and holes become quasi-free and are separated by the electric field applied, a discrete bound state most probably has alternative decay channels like luminescence, thus reducing the measured photocurrent at the line. A simple correction taking into account the losses due to the reflectivity at the lines cannot account for the depths of the minima in the photocurrent spectra.

The dip at about 11.6 eV in the photoconductivity excitation spectra (Fig. 2 and 3) is caused by the 5d'$(1\frac{1}{2})^o$ atomic peak, broadened and shifted due to molecular interactions. It should also be noted that the peak of the n' = 1 ($\Gamma\ (\frac{1}{2})$) exciton at about 9.45 eV is very close to the threshold

*The reflectivities were measured in Saint Etienne with the cooperation of J.L. Subtil

for the highest-density graph ("a") of Fig. 1 and therefore the shape of the threshold is probably modified for this density. At still higher liquid densities and in the solid the 9.45 eV discrete reflection peak appears as a pronounced dip in the photoconductivity excitation spectrum[2,10].

Comparison of the reflection spectra with the photoconductivity excitation spectra reveals another interesting point: the reflection peaks due to excitonic bands and the atomic lines modified by molecular interactions change in position very little with density[7,8] while the photoconductivity threshold changes considerably, moving to higher photon energies and decreasing in slope with decreasing density. The latter facts were stressed when discussing Fig. 2; the former one is also clearly illustrated in the same figure by the invariance of the position of the dip at 10.3 eV.

The structure in the photoconductivity excitation spectrum at and around 10.3 eV may easily cause a misinterpretation of the photoconductivity excitation spectra, especially for such densities, where the photoconduction threshold is very near to 10.3 eV. For example, curve "d" of Fig. 2 may be interpreted as involving two thresholds: a gradual one at about 10 eV and a much steeper one at about 10.35 eV and in fact, a preliminary brief report of the results[13] included the assumption of two thresholds. However, further considerations brought weightly arguments against such a presentation: a) the position and width of the dips is very close to that of the corresponding reflection bands (Fig. 2). b) If the threshold E_{pc} is taken to appear at the point where the current starts to rise, a continuous curve $E_{pc}(\rho_N)$ with a continuously varying derivative is obtained (Fig. 4). A quantitative support for this view should be furnished by knowing the absorption coefficient k(E) for photon energies at and around 10.3 eV; this

is being worked out by means of Kramers-Kronig analysis of reflective data for the LiF/Xe interface [14].

Usually, E_{pc} is determined from graphs of the kind presented in Fig. 2 by the intercepts of extrapolated straight portions of a power law: i_{ph}^{m} vs. E, m being mostly chosen to be either 1/2, 1 or 2 in accord with some theoretical model but often somewhat arbitrarily. On the other hand, defining E_{pc} as the start of the rising portion of the E_{pc} vs. hν graph has an intrinsic element of inaccuracy, especially if the noise level of the zero line is not negligible (e.g., graphs e and f in Fig. 2). For the data of Fig. 4 the photocurrent thresholds were determined by the latter method, taking the averages of two independent determinations. Very similar results were obtained if E_{pc} was determined from the intercept of the linear part of i_{ph}^{2} vs. hν plots. It is seen that at the highest densities E_{pc} = 9.19 eV. Previous determinations of the photoconductivity threshold in liquid xenon gave E_{pc} = 9.20 eV[2,10]. The difference stems from slightly different methods of determination[2,10] of E_{pc}. The increase of E_{pc} with decreasing density is seen to be monotonous, almost linear, down to a density[10] of about 4×10^{21} atoms/cm^3, and having a fasterrising portion at the lowest densities. E_{pc} extrapolates to 11.10 eV at zero density. This limit is equal to the difference between the energy minimum of the xenon molecular ion Xe_2^+ and the xenon atom ground state[1]. Transitions between the two states were shown to be possible[1] for all photon energies above 11.10 eV due to the Hornbeck-Molnar process[15] via an excimer state Xe_2^*, provided the density is larger than about 10^{19} atoms/cm^3.

In order to complete the picture on the evolution of electron energy band with density the ionization energy of the valence-band hole P^+ was evaluated as a function of the number density ρ_N. Following Messing and Jortner's work[16] on doped fluid argon the simple Born charging energy formula was used

$$P^+ = -\frac{e^2}{2\sigma}\left(1-\frac{1}{\epsilon}\right) \qquad \ldots\ldots 1$$

where e is the electron charge, σ = 0.39 nm is the calculated hard core radius of a xenon atom[17] and ϵ is the long-wavelength optical dielectric constant. Near the triple point the value of ϵ determined directly[18] was used; at other densities it was calculated using the triple-point value and the Clausius-Mossotti formula. The use of the simple formula can be justified as follows: Messing and Jortner showed[16] that the results of Eq. 1 for Xe-doped fluid argon are in accord within ± 10 % with results obtained by means of Lekner's screening function[19], taking into account values of pair correlation functions and the Kirkwood superposition approximation[20]. Experimental evidence for the reliability of both determinations of $P^+(\rho_N)$ came from comparison of directly measured values[9] of the quasi-free electron energy $V_o(\rho_N)$ in fluid argon with values based on the calculated $P^+(\rho_N)$values and spectroscopic evidence[16]. $P^+(\rho_N)$ as evaluated by means of Eq. 1 appears in Fig. 5; it is seen that $P^+ = 0$ for $\rho_N = 0$ and that $P^+(\rho_N)$ is an almost linear function. The highest value of $|P^+|$ obtained at the triple-point density, is about 0.9 eV. However, estimates of $|P^+|$ for solid xenon, obtained by different methods, yielded considerably higher values: 1.32 eV[21] and 1.39 eV[22] respectively. The

discrepancy is too large to attribute it to the change in ε due to the density change upon the phase transition: this effect would increase $|P^+|$ as determined from Eq. 1 only by about 10 %. Thus it is possible that the true values of $|P^+|$ are appreciably higher than indicated in Fig. 5.

Figure 6 summarizes the evolution of the band structure in fluid xenon on the basis of the above results. The zero line is the vacuum level. V_o is the energy of the free-electron state at the bottom of the conduction band (or, the electron affinity), reproduced from a previous publication[6]. The ionization energy of an electron at the top of the valence band

$$I_{TH} = -V_o + E_{pc}$$

is seen to decrease with increasing density though it stays roughly constant for densities between 5 and 10×10^{21} atoms/cm^3. The graph also includes $P^+ - I_{TH}$: this would be the ground state of a valence-band electron if there were no hole polarization effects as expressed by P^+. Apart from an initial rise at low densities this level seems to stay constant (within the experimental accuracy) for a wide density range. Apparently the results presented in Fig. 6 are the first case of any non-metal, crystalline or not, where the evolution of these band structure parameters was followed in detail.

3. Discussion

A. Photoconductivity; electron mobility and excitons

The similarity of values of several band structure parameters in solid xenon and in the corresponding liquid has been stressed repeatedly[2,4]. The continuous and gradual change of the level of the bottom of the conduction band, the level of the top of the valence band and the hole polarization energy P^+ with density found in this work indicated that there is no sudden change in the energy levels relevant to the electrical conduction. This is true down to densities of the order of 10^{21} atoms/cm^3: at this density region there is an increase in the slope $\left|\frac{dE_{pc}}{d\rho_N}\right|$ and the main contribution to the conductivity becomes that due to the Hornbeck-Molnar process[1]. It follows that the conduction in a solid-like conduction band persists down to very low densities where it changes continuously and gradually to gas-like conduction. This conclusion will now be discussed in comparison with the density dependence of the electron mobility[5] and of the exciton bands[7,8].

It was demonstrated by Huang and Freeman[5] in their work on the electron mobility of fluid xenon that the product of the number density by the zero-field mobility $\mu_o\rho_N$ is constant from zero density up to about $\rho_N = 2\times10^{20}$ atoms/cm^3. This is a typical behaviour of the zero-field mobility in a gas. Above this density there is a minimum in $\mu_o\rho_N$ (at $\sim 3\times10^{21}$ atoms/cm^3), attributed to[5] quasi-localization due to density fluctuations in the liquid. This minimum can be eliminated by a slight increase of the temperature, indicating that the potential well involved in the

localization is very shallow. The mobility is strongly dependent on the applied electric field F, but at any given field F, $\mu(F)$ varies slowly with density without sudden changes; $\mu(F)$ always has a minimum at about $\rho_N \sim 10^{21}$ atoms/cm^3.

The excitonic bands in fluid xenon (and krypton) behave differently. The $n' = 1$ ($\Gamma\ (\frac{1}{2})$) exciton appears only at densities above 2.7×10^{21} atoms/cm^3; the $n = 1$ ($\Gamma\ (\frac{3}{2})$) only above 4.9×10^{21} atoms/cm^3 and the $n = 2$ ($\Gamma\ (\frac{3}{2})$) exciton only above 10.8×10^{21} atoms/cm^3. In comparison, we note that below $\rho_N \sim 5 \times 10^{20}$ atoms/cm^3 $|dE_{pc}/d\rho_N|$ starts to increase steeply (Fig. 4) and that $\mu_o \rho_N$ deviates from its constant value at $\rho_N \sim 2 \times 10^{20}$ atoms/cm^3. Thus the exciton threshold densities are considerably above those which may indicate a transition from "gas-like" conduction to conduction in a conduction band ("solid-like"). A detailed study[7] of the evolution of the $n = 1$ ($\Gamma\ (\frac{3}{2})$) exciton indicated that for the appearance of such excitons light absorption has to take place in a cluster of at least 10 atoms occupying not more than a volume of 1.5 nm^3. If a similar condition would be necessary for "solid-like" conduction in an energy band as well, a rather sudden change of E_{pc} could be expected at such a density, where the individual clusters do not overlap sufficiently to form a conducting bridge between the electrodes. In other words, one might expect percolation effects at some density. The results of this work show no such effects.

The different behaviour of excitons and of electrons contributing to conduction can be readily understood following arguments by Basak and Cohen[23] leading to their multiple-scattering theory of mobility in fluid rare gases. The de Broglie wavelength λ_e for a thermalized electron at $T = 300^\circ$ K

turns out to be about 6 nm, if one assumes Boltzmann equipartition and thermal electron velocities. It is reasonable to postulate that as long as this wavelength is considerably larger than the average interatomic distance a, conduction electrons are not scatterd by individual atoms, but rather by density fluctuations. For $\rho_N = 10^{21}$ atoms/cm^3 $a = 1$ nm, so $\lambda_e/a = 6$; for all other densities discussed in this paper the ratio is even larger (up to ~ 14 near the triple point). Because of the large value of λ_e, the thermal or almost thermal conduction electron cannot be confined to a small cluster (typical dimension: ~ 1 nm) that is, indeed, capable of accommodating an exciton. Thus the energy at which the electron finds itself within the sample after it had been excited (i.e., V_o) is determined by properties averaged over many atoms. The transition to gas-like conduction, characterized by single scattering on individual atoms, occurs gradually for $\rho_N < 10^{21}$ atoms/cm^3, as the interatomic distance becomes comparable to λ_e.

Confinement of an exciton to a cluster does not constitute of course any difficulty, as the exciton energy is such as to ensure a λ_e-value consistent with the electron orbit.

B. Scattering mechanisms

Because of its much higher kinetic energy and confinement to orbit the electron belonging to an exciton may be subject to a different scattering mechanism than a more or less thermal free electron, especially if its Bohr radius is very small ($n = 1$ and $n' = 1$ excitons): in such a case

density fluctuations of the medium are irrelevant to scattering and single scattering processes have to be considered.

Some of the above considerations recall the paper by Rice and Jortner discussing the possible existence of Wannier excitons in simple liquids[24]. These authors gave a rough estimate for the minimum conditions at which such excitons may exist by requiring $\omega\tau_c >> 1$, ω being the angular frequency of the exciton and τ_c a scattering time that is in principle wave vector-dependent and is calculated by reckoning with scattering on the atoms of the liquid. Applying this condition to the observability of the $n = 2$ ($\Gamma\left(\frac{3}{2}\right)$) exciton in fluid xenon we reported[8] that for $\rho_N = 10.8\times10^{21}$ atoms/cm^3 (a density at which the exciton is just observable) $\omega\tau_c = 140$. Thus, it seemed that the condition $\omega\tau_c >> 1$ was satisfied rather too generously. However, in these considerations τ_c was estimated from the zero-field mobility, which is in practice determined by multiple-scattering[23], while for the high electron energy of the exciton (its radius is about 1 nm) single scattering is applicable. In other words it follows that τ_c for the electron confined to the exciton is much smaller than τ_c of the multiple scattering, determined by the zero- field mobility. Similarly, estimation of the width ΔE of the exciton band from the indeterminacy principle $\Delta E > h/\pi\tau_c$, h being Planck's constant, yields a factor of 40 between the two sides of the inequality if τ_c is taken from the zero-field mobility. This also points to the necessity of taking a considerably smaller value of τ_c into account for the electron belonging to the exciton.

C. Band gaps and the position of discrete transitions

Another interesting point of comparison between bound and quasi-free electrons is to consider the relative positions of excitonic and modified atomic peaks in comparison with the photoconductivity threshold E_{pc}. E_{pc} is equal to the energy difference between the bottom of the conduction band (V_o) and the top of the uppermost valence band (V_o-E_{pc}). The $\Gamma\left(\frac{3}{2}\right)$ exciton series is formed by the association of a conduction-band electron with a hole from this topmost valence band. Fig. 4 showed that E_{pc} varies considerably in the density range of 4.9 to 13.5×10^{21} atoms/cm^3, in which the $n = 1$ ($\Gamma\left(\frac{3}{2}\right)$) exciton discussed exists. In the same range there is, however, very little change in the position of the excitonic peak[8]. Such behaviour was predicted by W.B. Fowler[21] for excitons of small radius; according to his considerations, electronic polarization can be neglected for cases of excited states (excitons, F-centres, etc.) where the average radius of the orbit is considerably less than the interatomic distance. An indirect support for the validity of this approach was found by trying to use the one-electron approximation for the position E_1 of this exciton:

$$E_1 = E_G - G = E_{pc} - G = E_{pc} - \frac{13.6\ m^*}{\varepsilon^2} \qquad \ldots\ldots\ 2$$

G being the exciton binding energy in eV, m^* the reduced effective mass in terms of the free electron mass and ε the long-wavelength

optical dielectric constant. We checked the applicability of Eq.2 by substituting experimental values of E_1 and E_{pc} for the whole density range where the excitons are observed, using ε-values based on Sinnock and Smith's measurements[18] and the Clausius-Mossotti relation. This procedure yields m^* as a function of the density ρ_N. For the highest density of the range ($\sim 13.5\times10^{21}$ atoms/cm^3) $m^* = 0.26$, but this value went down to $m^* = 0.19$ for $\rho_N = 4.9\times10^{21}$ atoms/cm^3. This result does not seem meaningful, since if Eq. 2 were applicable for this exciton, m^* would stay either constant or else increase with decreasing density towards $m^* = 1$ in a very dilute gas. Thus Eq. 2 cannot be applied for the $n = 1$ ($\Gamma\left(\frac{3}{2}\right)$) exciton in a wide density range; it yields in solid xenon reasonable results that are consistent with higher levels of the $\Gamma\left(\frac{3}{2}\right)$ series because a fortuitous mutual cancelling of several central-cell corrections necessary for the calculation of the energy of this small-radius exciton[21,25,26].

The approximate constancy of position of the reflection peaks (some of them appearing as dips in the photoconductivity excitation spectrum) at 9.45, 10.16, 10.32 and 11.5 eV is explained on the same lines, with a correlary: Neither one of these peaks is due to an exciton formed by a conduction-band electron and a hole from the uppermost valence band, but they belong to deeper-lying valence bands or discrete levels. This explains the fact that E_{pc} may be smaller or larger than the energy of the peaks according to the density (Fig. 2).

D. Relations between band structure parameters and ionization potentials

It was stated near the end of the previous chapter that the calculated values of the hole polarization energy P^+ of Fig. 5 are definitely smaller in absolute value than those evaluated by other methods[21,22]. It is impossible to tell with certainty which calculations are the correct ones, but in any case there would be little difference in the general trend of these graphs.

Figure 6 shows that the energy of the top of the valence band $-I_{TH} = V_o - E_{pc}$ stays constant for a broad range of densities and the same is true about the energy $P^+ - I_{TH}$. This latter energy level is the ground state of a valence-band hole that would be obtained if there was no hole polarization energy P^+. Both $-I_{TH}$ and $P^+ - I_{TH}$ change considerably at low densities (below 3×10^{21} and 1×10^{21} atoms/cm^3 respectively). It is tempting to relate these changes to valence band formation from the $5p^6$ atomic cores with increasing density. It is hoped that the availability of these first experimental data on the evolution of energy bands should stimulate formulation of appropriate theories as well on this point.

It is seen in Fig. 6 that the low density limit of both $-I_{TH}$ and $P^+ - I_{TH}$ is very near to the adiabatic ionization potential of the xenon dimer[27] $I_{dimer} = 11.13$ eV. This fact is at first surprising, since the Franck-Condon principle would make very improbable direct transitions from the free atoms (or from the dimers) into the minimum of the configurational curve of the molecular ion, occurring

at the rather close distance of 0.285 nm[27]. However, we showed in Ref. 1 that such a transition is, indeed, very probable for densities higher than 10^{19} atoms/cm^3 and for all photon energies larger than the threshold I_{dimer}-$D(Xe_2)$, $D(Xe_2)$ being the dissociation energy ($D(Xe_2)$ = 0.024 eV[27]) of the Van der Waals molecule Xe_2. This is so because the Hornbeck-Molnar process appears for both at the maxima and in the wings of the atomic absorption lines. The ionization limit of the free atom I_G = 12.127 eV would thus become effective only at extremely low densities. Now the Hornbeck-Molnar process deals,in fact, with interactions of the excited states only: I_{dimer}-$D(Xe_2)$ would be an upper limit for the ionization energy even if there were no changes in the ground state, i.e., no polarization by the hole. In other words, P^+-I_{TH} must be equal or somewhat smaller than I_{dimer}-$D(Xe_2)$. When the valence bands are formed, a slight lattice polaron effect may also occur[21] that would account for small differences.

4. Acknowledgements

The authors wish to express their thanks to several institutions (DESY, DAAD and the Israel Commission for Basic Research) for their contributions towards the success of this project. Among numerous individuals we specially thank Mr. W. Jark, Dipl.-Phys. of Hamburg University, for valuable technical help.

References

1. P. Laporte, V. Saile, R. Reininger, U. Asaf and I.T. Steinberger, Phys. Rev. A, in press
2. U. Asaf and I.T. Steinberger, Phys. Rev. B10, 4464 (1974)
3. L.S. Miller, S. Howe and W.E. Spear, Phys. Rev. 166, 871 (1968)
4. I.T. Steinberger and U. Asaf, Phys. Rev. B8, 914 (1973)
5. S.S.S. Huang and G.R. Freeman, J. Chem. Phys. 68(4), 1355 (1978)
6. R. Reininger, U. Asaf and I.T. Steinberger, Chem. Phys. Letters, in press
7. P. Laporte and I.T. Steinberger, Phys. Rev. B15, 2583 (1977)
8. P. Laporte, J.L. Subtil, U. Asaf, I.T. Steinberger and S. Wind, Phys. Rev. Letters 45, 2138 (1980)
9. R. Reininger, U. Asaf and I.T. Steinberger, Phys. Rev. B, in press
10. R. Reininger, U. Asaf, P. Laporte and I.T. Steinberger, in Proceedings of the Seventh International Conference on Conduction and Breakdown in Dielectric Liquids, edited by W.F. Schmidt (Berlin, 1981), p. 69; J. Electrostatics 12, 123 (1982)
11. V. Saile, G. Gürtler, E.E. Koch, A. Kozevnikov, M. Skibowski and W. Steinmann, Appl. Optics 15, 2559 (1976)
12. P. Laporte, J.L. Subtil, M. Bon and H. Damany, Appl. Optics 20, 2133 (1981)
13. R. Reininger, U. Asaf, P. Laporte, V. Saile and I.T. Steinberger, Bull. Israel Phys. Soc. 28, 21 (1982)
14. P. Laporte and J.L. Subtil, to be published
15. J.A. Hornbeck and J.P. Molnar, Phys. Rev. 84, 621 (1951)
16. I. Messing and J. Jortner, Chem. Phys. 24, 183 (1979)
17. N.W. Ashcroft, Physica 35, 148 (1967)
18. A.C. Sinnock and B.L. Smith, Phys. Rev. 181, 1297 (1969)
19. J. Lekner, Phys. Rev. 158, 130 (1967)
20. J. G. Kirkwood, J. Chem. Phys. 3, 300 (1935)
21. W.B. Fowler, Phys. Rev. 151, 657 (1966)
22. L.E. Lyons and M.G. Sceats, Chem. Phys. Lett. 6, 217 (1970)
23. S. Basak and M.H. Cohen, Phys. Rev. B20, 3404 (1979)
24. S.A. Rice and J. Jortner, J. Chem. Phys. 44, 4470 (1970)
25. J. Hermanson and J.C. Phillips, Phys. Rev. 150, 652 (1966)
26. J. Hermanson, Phys. Rev. 150, 660 (1966)
27. C.Y. Ng, D.J.Trevor, B.H. Mahan and Y.T. Lee, J. Chem. Phys. 65, 4327 (1976)

Figure Captions

Figure 1 Cross section of the sample cell. A - retaining ring; B and F - parts of "Conflat" seal; C - LiF window, glued to B; D - copper gasket; E - spring and contact head; G - filling tube; H - ceramic insulator of ultra-high vacuum feedthrough; I - central stalk welded into the feedthrough. The cell has two feedthroughs, but for simplicity only one is drawn.

Figure 2 Normalized photocurrent as a function of the energy of incident photons at various number densities (10^{21} atoms/cm^3) a-10.9; b-8.3; c-6.2; d-4.1; e-3.3; f-2.3.

Figure 3 Normalized photocurrent compared with the reflectance of the xenon/MgF_2 interface at similar densities.

Figure 4 The density dependence of the photoconductivity threshold.

Figure 5 The calculated density dependence of the hole polarization energy P^+. See text.

Figure 6 Density dependence of energy band parameters.

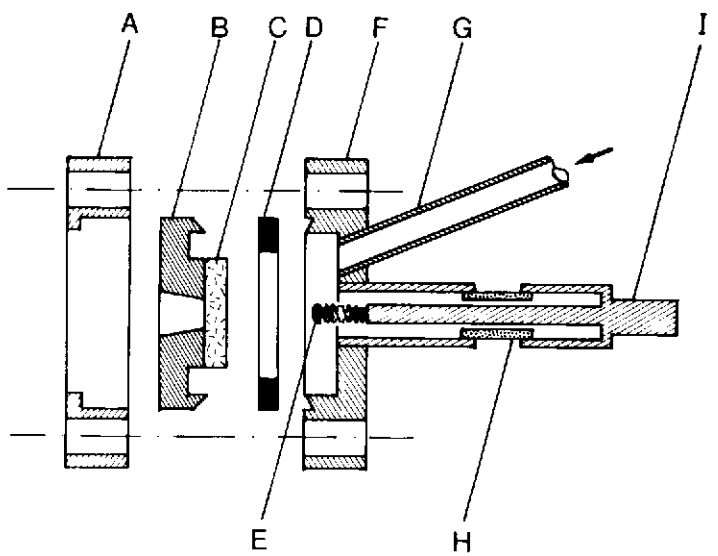

Fig. 1

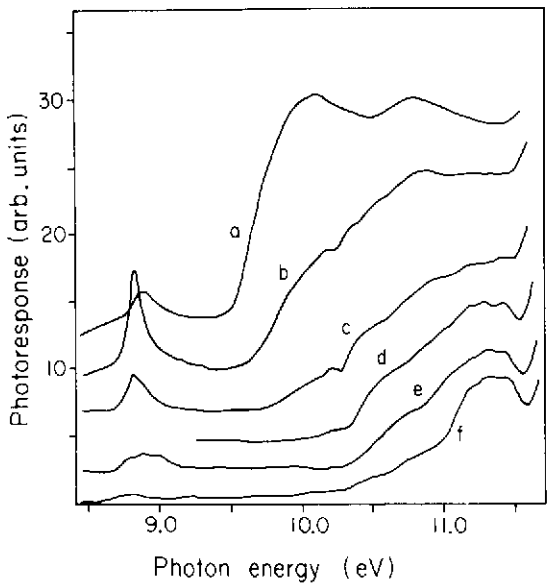
Photoresponse (arb. units)
30
20
10
a
b
c
d
e
f
9.0
10.0
11.0
Photon energy (eV)

Fig. 2

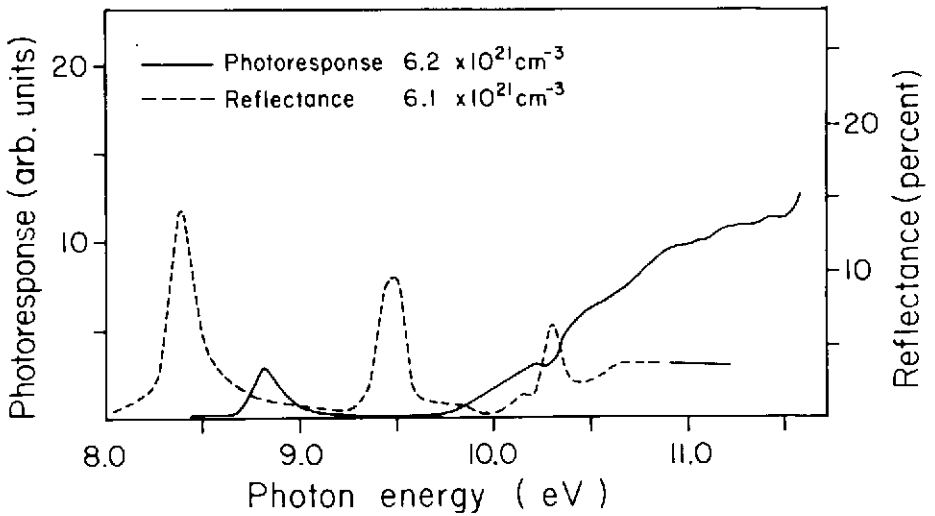
Photoresponse 6.2 x10²¹cm⁻³
Reflectance 6.1 x10²¹cm⁻³
Photoresponse (arb. units)
20
10
Reflectance (percent)
20
10
8.0
9.0
10.0
11.0
Photon energy (eV)

Fig. 3

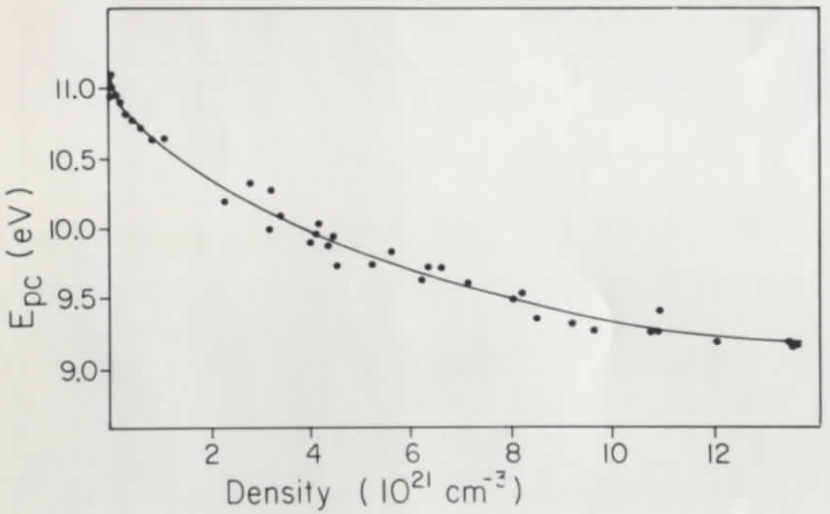
11.0
10.5
10.0
9.5
9.0
E_{pc} (eV)
2
4
6
8
10
12
Density (10^{21} cm^{-3})

Fig. 4

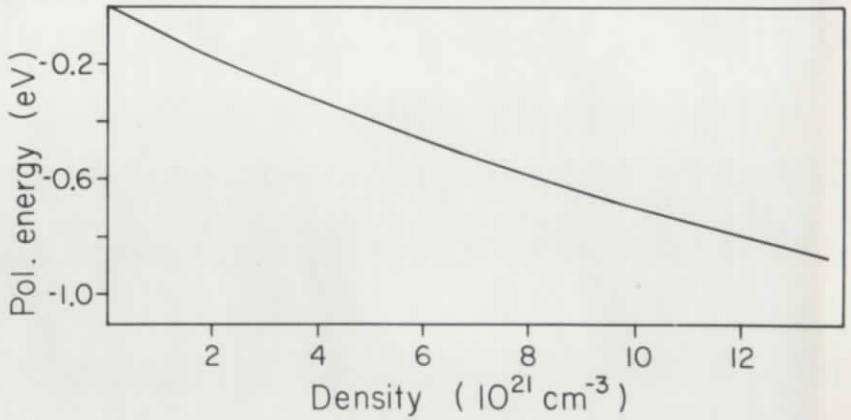
-0.2
-0.6
-1.0
Pol. energy (eV)
2
4
6
8
10
12
Density (10^{21} cm^{-3})

Fig. 5

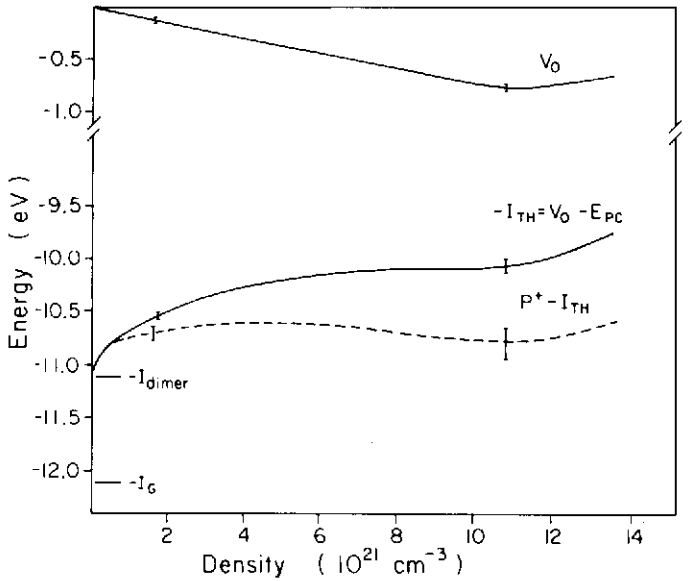
-0.5
-1.0
-9.5
-10.0
-10.5
-11.0
-11.5
-12.0
Energy (eV)
V_0
$-I_{TH}=V_0-E_{PC}$
P^+-I_{TH}
$-I$
$-I_{dimer}$
$-I_G$
2
4
6
8
10
12
14
Density (10^{21} cm^{-3})

Fig. 6